

## Thermal and Viscoelastic Properties of $\kappa/\iota$ -Hybrid Carrageenan Gels Obtained from the Portuguese Seaweed *Mastocarpus stellatus*

L. HILLIOU,\* F. D. S. LAROTONDA, A. M. SERENO, AND M. P. GONÇALVES

REQUIMTE-CEQUP, Departamento de Engenharia Química, Faculdade de Engenharia da Universidade do Porto, Rua Dr. Roberto Frias, s/n, 4200-465 Porto, Portugal

The potential use of the underexploited Portuguese seaweed *Mastocarpus stellatus* as a source of natural thickening and gelling agents for food applications has been investigated. The alkaline pretreatment duration and extraction parameters (pH, temperature, and extraction duration) of seaweeds have been systematically varied in order to produce  $\kappa/\iota$ -hybrid carrageenans exhibiting a wide range of chemical properties. The mechanical spectra and the setting and melting temperatures of gels obtained by cooling 1.5 wt % extracted biopolymers solutions in 0.05 mol/dm<sup>3</sup> KCl were measured by means of small amplitude oscillatory shear experiments. Gels showing elastic storage moduli ranging from 250 to 2750 Pa with no water syneresis could be obtained, and the relationships between the thermal properties and elasticity of the gels were evidenced. Gels mechanical properties are shown to correlate well with polysaccharides chemical parameters such as the degree of sulfate groups, the molecular weight distribution, and the relative content in  $\iota$ -carrageenan monomers as determined by FTIR spectroscopy.

**KEYWORDS:** *Mastocarpus stellatus*;  $\kappa/\iota$ -hybrid carrageenan; chemical structure; gel viscoelasticity

### 1. INTRODUCTION

Carrageenan is a generic name given to a family of sulfated polysaccharides isolated from red seaweeds (1). These water-soluble linear biopolymers are increasingly used as natural thickeners, formulation stabilizers, or gelling agents in applications ranging from food industry (mainly dairy products) to pharmaceuticals (2). Carrageenan is classified in three industrially relevant types:  $\lambda$ -carrageenan, which is a highly sulfated galactan with viscosity enhancer properties;  $\iota$ -carrageenan, which forms thermoreversible soft gels; and  $\kappa$ -carrageenan, which gives strong and brittle gels with water syneresis. But in reality, carrageenan biopolymers possess a complex hybrid chemical structure comprising  $\lambda$ -,  $\iota$ -, or  $\kappa$ -carrageenan monomers together with nongelling biological precursor monomers such as  $\nu$ - or  $\mu$ -carrageenan monomers (3). The relative amounts of gelling or nongelling monomers depend on the algal source from which they are obtained (2–4), as well as on the extraction procedure used to recover the biopolymers (5). Demand for carrageenan is steadily rising as new nonfood applications are encountered, and manufacturers are pressed to screen the potential of new natural resources or new chemical processing for the production of carrageenan with preferentially good gelling properties. This also boosted the research efforts witnessed during the past decade or so. A wide set of experimental techniques were utilized for the structural investigation (6–8) and characterizing

the dynamical (9–11) and rheological (12, 13) properties of gelling carrageenans, thus contributing to a better fundamental understanding of the gel mechanisms. The now widely accepted picture emerging from this intensive research is that gelation results from the salt-induced or temperature-induced aggregation of helical conformers. The internal aggregates structure and the aggregates three-dimensional network that give rise to elasticity depend on both carrageenan type and the salt used to promote or stabilize the clusters. Consequently, gels can be obtained that offer a wide variety of elastic and thermal properties ranging from weak gels to strong gels presenting syneresis.

However, all these studies dealt with model carrageenans virtually made of a single type of monomer, thus presenting chemical structures very similar to ideal  $\iota$ - or  $\kappa$ -carrageenan homopolymers. Only very recently,  $\kappa/\iota$ -hybrid carrageenans, essentially made of blocks of  $\iota$ - and  $\kappa$ -carrageenan monomers, have received a renewed interest (14–17), as they are most naturally frequent in seaweeds used for carrageenan production and because they present unique functional properties when compared to ideal carrageenan homopolymers (18, 19). These properties are evidently caused by the copolymer structure of these hybrid carrageenans, but the interplay between chemical structure and gel thermoviscoelastic properties or gelling mechanism still needs to be documented. We lately started working along this line of research, focusing our attention on the biopolymers extracted from the underexploited Portuguese seaweed *Mastocarpus stellatus*, which are a known source of  $\kappa/\iota$ -hybrid carrageenans (4). The biopolymer chemical structure

\* Corresponding author. Phone: (+351) 22 508 1686. FAX: (+351) 22 508 1449. E-mail: hilliou@fe.up.pt.

can be tuned by the careful control of extraction parameters and alkaline pretreatment conditions, thus allowing the delivery of biopolymers with different  $\iota$ - and  $\kappa$ -carrageenan monomer compositions as well as molecular weight distributions (20). In this paper, the thermal and viscoelastic properties of  $\kappa/\iota$ -hybrid carrageenans gels are presented. Small amplitude oscillatory shear experiments show that gels exhibiting elastic storage moduli ranging from 250 to 2750 Pa with no water syneresis and gel melting temperatures ranging from 41 to 52 °C can be obtained by cooling hot  $\kappa/\iota$ -hybrid carrageenan solutions in 0.05 mol/dm<sup>3</sup> KCl salt down to 20 °C. Mechanical spectra recorded on equilibrated gels and gel thermal hysteresis suggest that  $\kappa/\iota$ -hybrid carrageenan copolymers build a space-filling network that is structurally reminiscent of the ones formed by ideal  $\kappa$ -carrageenan homopolymers. This structural feature is explained by the chemical structure, which primarily contains  $\kappa$ -carrageenan monomers. Gels elastic properties correlate well with the chemical parameters of the biopolymers, such as the molecular weight distribution, the overall degree of sulfate groups determined by a newly introduced FTIR intensity ratio, and the relative content in  $\iota$ -carrageenan monomers as determined by FTIR spectroscopy.

## 2. MATERIALS AND METHODS

**2.1. Seaweeds Sampling and Alkaline Pretreatment.** *M. stellatus* seaweeds were hand-collected during May 2004 on the northern coast of Portugal (Vila Praia de Ancora). No attempt was made to separate algal specimen with different life phases (female or male gametophytes, and carposporophytes). Seaweeds were first washed several times with tap water in order to remove nonalgal materials. An alkali pretreatment (200 g of wet algae in 8 dm<sup>3</sup> of 0.1 mol/dm<sup>3</sup> Na<sub>2</sub>CO<sub>3</sub> at room temperature) was then performed during a time (PT) varying between 20 and 70 h, in order to likely convert the carrageenan biological precursors into gelling carrageenan monomers (1, 5, 20). Excess sodium salt was removed after alkaline pretreatment by washing the seaweeds several times until the bathing water reached a pH of 7. Then, the seaweeds were dried at 60 °C for 48 h in a ventilated oven and stored at room temperature.

**2.2. Biopolymer Extraction.** Carrageenan extraction (40 g of dried alga in 4 dm<sup>3</sup> of tap water) was performed at a temperature ( $T$ ) during a time ( $t$ ) and at a pH value monitored by the addition of 0.1 mol/dm<sup>3</sup> NaOH or 0.01 mol/dm<sup>3</sup> HCl. Parameters  $T$ ,  $t$ , and pH were separately varied from 80 to 110 °C, from 30 min to 4 h, and from 7 to 9, respectively. The extract was then filtered with metallic screens followed by cotton clothes prior to water evaporation performed at 60 °C. The resulting concentrated extract was then precipitated in ethanol (95%). The precipitate was separated from the water–ethanol mixture by filtration and the recovered polysaccharide was washed with further ethanol. The product was then dried at 60 °C under vacuum and milled. The resulting powder was purified by mixing in hot distilled water during 1 h and subsequent centrifugation performed at  $2 \times 10^4$  rpm and 38 °C during 40 min. The supernatant was finally recovered and dried at 60 °C under vacuum until constant weight was reached. Selected extractions were performed in triplicate in order to check the good qualitative reproducibility in the carrageenan gelling properties and to determine the experimental error (error bars in Figures 8 and 9) in the characterization of the corresponding biopolymer chemical structure and in the extraction yields (calculated on a dry basis) displayed in Table 1 together with the extraction parameters used during the recovery of all  $\kappa/\iota$ -hybrid carrageenans.

**2.3. Determination of the Chemical Structures and Molecular Weight Distributions of Extracted  $\kappa/\iota$ -Hybrid Carrageenans.** Fourier transform infrared spectroscopy (FTIR) and <sup>1</sup>H NMR spectroscopy were employed to assess the chemical structure of the extracted phycocolloids. Details about the chemical characterization can be found elsewhere (20). FTIR spectra were recorded with a Perkin-Elmer 157G infrared spectrometer and experiments were carried out with carrageenan films cast from dilute water solutions. The <sup>1</sup>H NMR spectra were

**Table 1.** Alkaline Pretreatment Duration (PT), Extraction Temperature ( $T$ ), Extraction pH, and Extraction Duration ( $t$ ) Used To Obtain the  $\kappa/\iota$ -hybrid Carrageenans Samples from *M. stellatus* Seaweeds

sample label	PT (h)	$T$ (°C)	pH	$t$ (h)	yield <sup>a</sup> (%)
M9	42	95	8	2	17 ± 1
M11	72	95	8	2	14 ± 0.5
M12	48	95	7	2	23 ± 1
M16	20	95	8	2	27 ± 2
M17	48	95	9	2	47 ± 5
M18	48	80	8	2	19 ± 1
M20	48	110	8	2	23
M23	48	95	8	0.5	13
M24	48	95	8	1	17 ± 2
M25	48	95	8	2	20
M26	48	95	8	4	25 ± 1

<sup>a</sup> Corresponding extraction yields are given and calculated from the ratio of dry carrageenan weight over dry seaweeds weight.

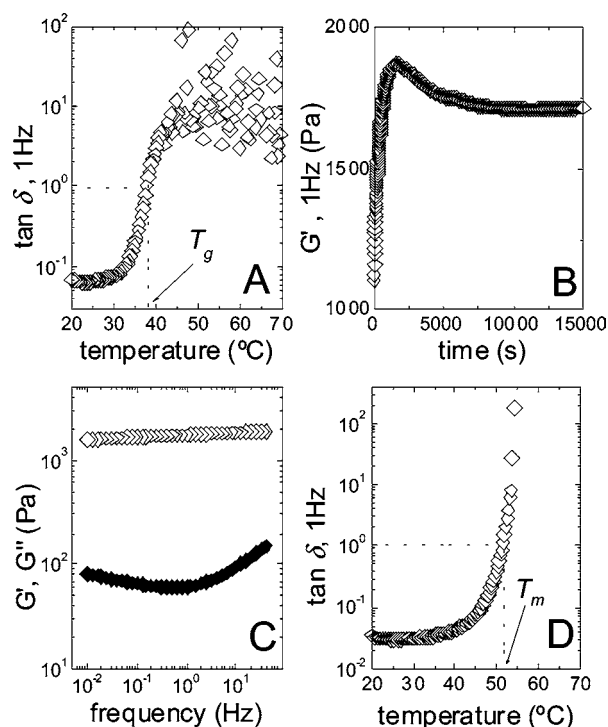


**Figure 1.** Experimental protocol used for the rheological characterization of  $\kappa/\iota$ -hybrid carrageenan gels. Dotted lines in A indicate the gel point  $T_g$ . Dotted lines in D indicate the gel melting temperature  $T_m$ . See Materials and Methods for details.

recorded on biopolymers dissolved in D<sub>2</sub>O and experiments were performed at 80 °C, on a Bruker ARX 400 NMR spectrometer (400 MHz), using TMS-PSA as internal standard. Number and weight average molecular weights,  $M_n$  and  $M_w$ , respectively, were obtained by size exclusion chromatography (Waters Co. apparatus equipped with a Waters Ultrahydrogel Linear column and a Waters 2410 differential refractive index detector) performed with 0.1% w/w carrageenan solutions in 0.1 mol/dm<sup>3</sup> NaCl at 40 °C. Under such salt, temperature, and concentration conditions, optical rotation experiments (14) indicate that  $\kappa/\iota$ -hybrid carrageenans showing similar chemical composition are in the coil conformation. This conformation is explained by the presence of biological carrageenan precursor monomers that prevent the formation of regular helical conformations. Details about the molecular weight distribution determination can be found elsewhere (20).

**2.2. Gel Thermal and Mechanical Characterization.** Figure 1 illustrates the experimental protocol used to characterize the gel setting temperature ( $T_g$ ), the gel melting temperature ( $T_m$ ), and the gel viscoelastic properties of all extracted  $\kappa/\iota$ -hybrid carrageenans (data

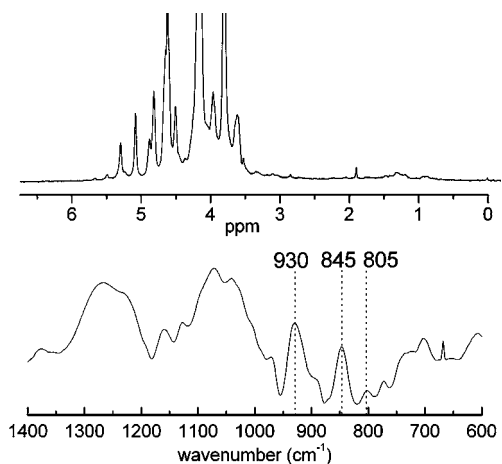


**Figure 2.** Chemical identification of the biopolymer extracted from *M. stellatus*:  $^1\text{H}$  NMR spectrum (top) and FTIR spectrum (bottom) of sample M26 obtained after 4 h of extraction at pH 8 and  $T = 95\text{ }^\circ\text{C}$  performed on alkali-treated (48 h) seaweeds.

for sample M11 are reported in **Figure 1**). Hot carrageenan solutions (1.5% w/w biopolymer in  $0.05\text{ mol/dm}^3$  KCl) were loaded at  $90\text{ }^\circ\text{C}$  in the preheated plate–plate geometry of a stress-controlled rheometer (AR2000, TA Instruments). Water loss was avoided by covering the geometry with paraffin oil. Hot solutions were first cooled ( $5\text{ }^\circ\text{C/min}$ ) down to  $20\text{ }^\circ\text{C}$  while small amplitude oscillatory shear strain with 0.1% amplitude was applied at 1 Hz in order to probe the temperature evolution of linear viscoelastic properties such as  $\tan\delta$ , the tangent of the phase shift angle  $\delta$  between imposed sinusoidal strain and measured sinusoidal stress (see **Figure 1A**). The point for which  $\tan\delta = 1$  was defined as the gel-setting temperature. We note here that the Winter–Chambon criterion (21) for liquid–solid transition determination could not be used, as the time evolution of dynamic moduli was too fast at temperatures close to the liquid–solid transition and did not allow proper measurement of mechanical spectra on a sufficiently wide frequency range. The time evolution of the storage modulus  $G'$  and the loss modulus  $G''$  was followed at  $20\text{ }^\circ\text{C}$  (0.1% strain at 1 Hz), allowing the determination of gel equilibrium conditions (**Figure 1B**). Equilibrated gels mechanical spectra were then measured in the linear regime by performing frequency sweeps with a 0.1% strain (see **Figure 1C**). From this test, one can extract the value of the gel storage modulus  $G'$  at 1 Hz ( $G_0$ ), which essentially mirrors the gel elasticity at equilibrium and  $20\text{ }^\circ\text{C}$ . Finally, the gels were heated ( $5\text{ }^\circ\text{C/min}$ ) up to  $90\text{ }^\circ\text{C}$  and  $G'$  and  $G''$  were simultaneously measured at a 0.1% strain and a frequency of 1 Hz, enabling the characterization of the gel melting point (see chart D) again defined as the temperature for which  $\tan\delta = 1$ .

### 3. RESULTS

**3.1. Chemical Characterization of the Hydrocolloid Extracted from *M. stellatus*.** The  $^1\text{H}$  NMR spectrum and FTIR spectrum of sample M26 isolated from alkali-treated (during 48 h) *M. stellatus* seaweeds after 4 h extraction performed at  $T = 95\text{ }^\circ\text{C}$  and at pH 8 are presented in **Figure 2**. Of special interest in the  $^1\text{H}$  NMR spectrum are the peaks showing up at 5.11 and 5.32 ppm, which are usually assigned (2) to  $\kappa$ -carrageenan and  $\iota$ -carrageenan monomers, respectively. An additional peak located at 5.52 ppm can be resolved, together with a shoulder appearing around 5.26 ppm. These two signals originate from biological carrageenan precursor monomers  $\nu$  and  $\mu$ , respectively. These precursors should normally be converted into  $\iota$ -carrageenan and  $\kappa$ -carrageenan monomers, respectively, by the alkali treatment. Indeed, for *M. stellatus* seaweeds, a dedicated study (20) demonstrated that the alkaline treatment should at least last for 20 h for an effective conversion of biological precursors, as inferred from the drop in  $^1\text{H}$  NMR

shoulder intensities resolved at 5.26 ppm. However, alkaline treatments with duration as long as 78 h were not sufficient for achieving a complete conversion. As a consequence, signals corresponding to  $\mu$ - and  $\nu$ -carrageenan monomers are still resolved in the  $^1\text{H}$  NMR spectrum of sample M26.

The FTIR spectrum in **Figure 2** confirms the complex structure of the extracted biopolymer, whose main spectral assets are indicated by three vertical dotted lines: an absorption band at  $805\text{ cm}^{-1}$  reminiscent of  $\iota$ -carrageenan monomers (22); a stronger band at  $930\text{ cm}^{-1}$ , which is a common feature of both  $\kappa$ - and  $\iota$ -monomers (23); and a band at  $845\text{ cm}^{-1}$ , which is reported to be specific to  $\kappa$ -,  $\iota$ -,  $\nu$ -, and  $\mu$ -monomers (4) as it relates to the COS group located on the fourth carbon of the galactose. These results are in harmony with a recent report on  $\kappa/\iota$ -hybrid carrageenans extracted from gametophyte samples of similar seaweeds collected on the northern coast of Portugal (22). Furthermore, KCl fractionation carried out in a separate study (20) demonstrates that  $\kappa$ -carrageenan biopolymers cannot be separated from  $\iota$ -carrageenan biopolymers. Instead, either an homogeneous viscous solution, a transparent gel, or a grainy, turbid gel (when KCl concentrations in excess of  $0.1\text{ mol/dm}^3$  and biopolymer concentrations above 1.5% w/w are used) is obtained after centrifugation. This is indicative of the copolymer nature (14) of the  $\kappa/\iota$ -hybrid carrageenan extracted from *M. stellatus*, which is to be seen as a macromolecular chain containing long sequences of  $\kappa$ - and  $\iota$ -carrageenan monomers (with sufficient length for allowing the formation of aggregating helices) separated by shorter sequences and/or units of  $\nu$ - and  $\mu$ -carrageenan monomers, rather than a mixture of essentially ideal  $\kappa$ -carrageenan and  $\iota$ -carrageenan biopolymers.

**3.2. Mechanical Properties of  $\kappa/\iota$ -Hybrid Carrageenan Gels.** Gels obtained by cooling  $\kappa/\iota$ -hybrid carrageenan hot solutions down to  $20\text{ }^\circ\text{C}$  need more than 3 h to reach equilibrium at this temperature, as illustrated by the time evolution of the storage shear modulus  $G'$  measured at 1 Hz and presented in chart B of **Figure 1**. Shortly after reaching  $20\text{ }^\circ\text{C}$ , the gel elasticity rapidly increases up to a maximum before slowly decaying down to its equilibrium value. Similar gel kinetics has been measured with mixtures of ideal  $\kappa$ -carrageenan and  $\iota$ -carrageenan homopolymers (24) and with ideal  $\iota$ -carrageenan homopolymers (6). Microstructural investigations (6, 25) carried out at different times during equilibration evidenced a structural rearrangement of the three-dimensional network responsible for the water syneresis that accompanies the gel kinetics. Visual inspection of  $\kappa/\iota$ -hybrid carrageenan gels equilibrated at  $20\text{ }^\circ\text{C}$  during 24 h in sealed plastic cups shows that the gels do not release any water during equilibration. To further test the hypothesis that shearing plates can stress the building gel and force trapped water to migrate toward the gel–plate interfaces, the experiment depicted in **Figure 1** was repeated with serrated plates. A comparison of the gel kinetics measured with the two shearing plates on sample M11 is provided in **Figure 3**. The good qualitative reproducibility of both gel kinetics (**Figure 3A**) and gel equilibrium mechanical spectra (**Figure 3B**) rules out the syneresis of water during gel equilibration. We are therefore left with the structural rearrangement of the gel network as an explanation for the observed gel kinetics. A data analysis inspired from Fourier transform rheology concepts (26) is proposed in **Figure 4** in order to check whether the structural evolution is induced by the 0.1% strain used during the mechanical testing or is an intrinsic gel building up. Any strain-induced structure or damage developing in the  $\kappa$ -hybrid carrageenan gels is reflected by some nonsinusoidal components (nonlinearity) showing up in the measured stress response to

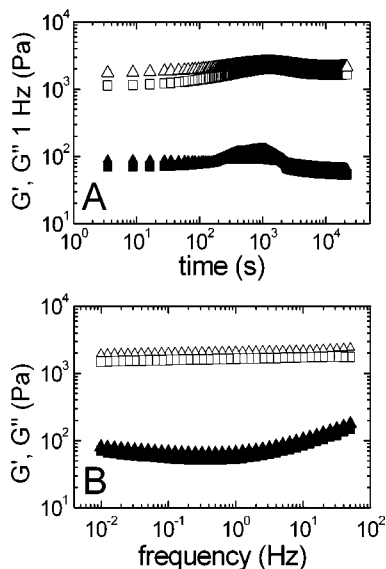


**Figure 3.** Effect of shearing plates surfaces (squares, serrated plates; triangles, smooth plates) on the reproducibility of experimental data collected for sample M11 at 20 °C. (A) Time dependence of the storage modulus (open symbols) and loss modulus (solid symbols) measured at 1 Hz. (B) Frequency dependence of storage and loss moduli (same symbols as in A) measured on the equilibrated gels at 20 °C.

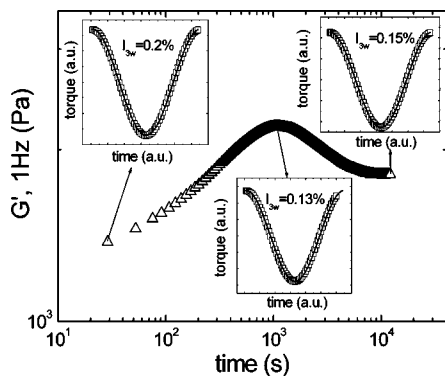


**Figure 4.** Analysis of the linearity of the stress response measured during equilibration at 20 °C of a  $\kappa/\iota$ -hybrid carrageenan gel (sample M24). In the insets, lines are the fits of eq 1 to the stress data ( $\square$ ) recorded at selected times (indicated by arrows) during the gel kinetics.

the imposed sinusoidal strain. Signal nonlinearity can be, to a first approximation, estimated by fitting the experimental data to the following periodic function

$$\sigma(t) = A \sin(\omega t) + AI_{3w} \sin(3\omega t + \phi_{3w}) \quad (1)$$

where  $A$  is the amplitude of the signal measured at a frequency  $\omega = 1$  Hz (the excitation frequency),  $I_{3w}$  is the scaled amplitude of the nonlinearity showing up at the third harmonic with phase shift  $\phi_{3w}$ . In the insets of **Figure 4**, where the time evolution of the gel storage modulus  $G'$  measured with sample M24 is presented, the stress data are displayed at different times during the gel kinetics, together with the corresponding fits obtained with eq 1 using the reported  $I_{3w}$  values. This satisfactory data analysis (standard errors of 10% were typically observed for all the  $I_{3w}$  values obtained with the fitting procedure, which is acceptable, given the neglect of higher harmonics needed to fully describe a nonsinusoidal waveform) demonstrates that the stress third harmonic scaled amplitude keeps values below 0.2%. The latter are smaller than the  $I_{3w}$  parameters calculated for all the corresponding strain signals throughout the duration of the

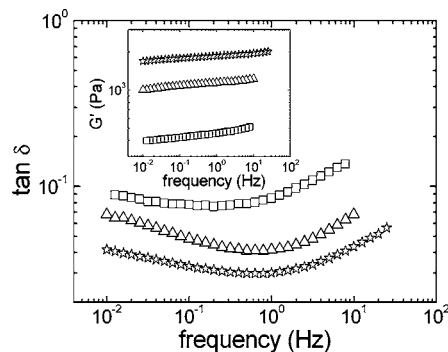


**Figure 5.** Frequency dependence of the tangent of mechanical phase shift angle  $\delta$  for equilibrated gels formed at 20 °C with samples M16 ( $\square$ ), M9 ( $\Delta$ ), and M26 ( $\square$ ). Inset: frequency dependence of corresponding gels storage moduli  $G'$ .

experiment. In other words, the rather small torque nonlinearity originates from the nonlinear deformation imposed by the rheometer (possibly caused by the use of pseudo-strain controlled experiments) and not from any strain-induced damaging of the gels. On the contrary, the time evolution of  $G'$  evidenced in **Figures 3** and **4** may rather originate from intrinsic structural rearrangements taking place during the equilibration of  $\kappa/\iota$ -hybrid carrageenan gels at 20 °C (see the discussion below).

Examples of mechanical spectra measured on equilibrated gels are presented in **Figure 5**. Qualitatively similar viscoelastic behaviors were observed with the remaining  $\kappa/\iota$ -hybrid carrageenans listed in **Table 1**. For the three gels depicted in **Figure 5**, the frequency dependence of the tangent of the phase shift angle  $\delta$  ( $\tan \delta = G''/G'$ ) shows a minimum, which suggests the existence of two relaxation times located at frequencies higher and smaller than the experimentally accessible frequencies. Comparison of storage moduli  $G'$  plotted in the inset of **Figure 5** with  $\tan \delta$  data reveals that increased gel strength (higher  $G'$ ) correlates with increased elastic properties (smaller  $\tan \delta$ ). This increase in gel elasticity is accompanied by a shift in the location of the  $\tan \delta$  minimum toward higher frequencies and a flattening of the shift angle frequency dependence. The observed flattening is indicative of the widening of the time distribution of the relaxation processes. In a recent study on gels made with ideal  $\kappa$ -carrageenans in 0.1 mol/dm<sup>3</sup> NaCl, Meunier et al. (9) measured mechanical spectra very similar to the ones shown in **Figure 5**: this suggests that the gels made from  $\kappa/\iota$ -hybrid carrageenans structurally resemble the gels made with pure  $\kappa$ -carrageenans. In contrast to these features, weak gels obtained from nonaggregating  $\kappa$ -carrageenan in NaI salt (12) as well as gels made with ideal  $\iota$ -carrageenans (13) both show  $G'$  and  $G''$  moduli with very weak frequency dependences.

**3.3. Interplay between Gels Thermal Properties and Gels Elasticity.** The gel-setting temperatures ( $T_g$ ) and the gel thermal hysteresis ( $\Delta T$ , calculated as  $\Delta T = T_m - T_g$ ) are plotted in **Figure 6** as a function of their corresponding gel equilibrium storage modulus  $G_0$  measured at 20 °C for all  $\kappa/\iota$ -hybrid carrageenan samples listed in **Table 1**.  $T_g$  and  $\Delta T$  are increasing functions of  $G_0$ . However, both thermal properties seem to level-off for  $G_0$  values higher than 1500 Pa. The data representation proposed in **Figure 6** suggests that gel thermal properties are closely related to gel elastic properties: stronger gels are easier to form (their gel-setting temperatures are higher) and melt at higher temperatures. Thermal hysteresis is usually reported as a  $\kappa$ -carrageenan gel fingerprint (1, 11) and is associated with the existence of big aggregates of helical conformers (10) exhibiting melting temperatures  $T_m$  higher than the temperature  $T_g$  at which smaller aggregates start to percolate to form a three-

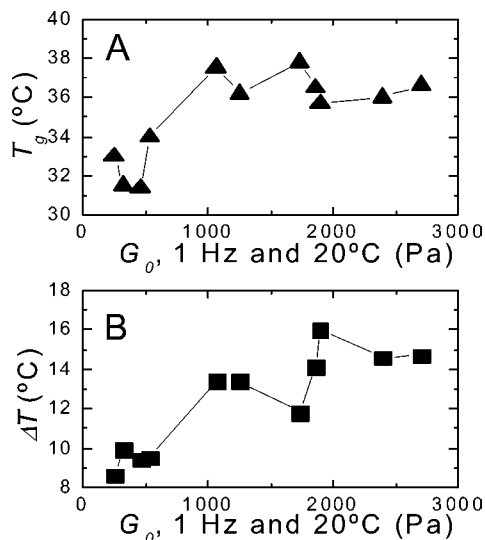


**Figure 6.** Relationship between gels thermal properties and gel elastic properties at 20 °C. (A) Gel-setting temperature  $T_g$  as a function of the corresponding gel elastic modulus  $G_0$ . (B) Thermal hysteresis  $\Delta T$  as a function of the corresponding gel elastic modulus  $G_0$ .

dimensional elastic network. The widely accepted gel mechanism (1–3, 5–12) for  $\kappa$ -carrageenans provides a good explanation for the interplay between thermal and mechanical behaviors: as more helices are bundled to form a mechanically effective cluster, the latter becomes more elastic, since the density of cross-links inside the aggregate is raised, and higher temperatures are needed to disrupt the bundles of helices.  $T_g$  and  $T_m$  values measured in the present study for the whole set of extracted  $\kappa/\iota$ -hybrid carrageenans are in fairly good agreement with values recently reported (17) for a commercial  $\kappa/\iota$ -hybrid carrageenan containing 50%  $\kappa$ -carrageenan monomers. A final comment on the thermal properties of the  $\kappa/\iota$ -hybrid carrageenan gels extracted from *M. stellatus* deals here with the monotonic decrease or increase of  $\tan \delta$  observed during the cooling (Figure 1A) or the heating (Figure 1D), respectively, of all samples listed in Table 1. Such smooth temperature dependences contrast with the thermal behavior measured some time ago by Parker et al. (24) for a mixture of  $\kappa$ -carrageenan and  $\iota$ -carrageenan under similar salt conditions. The authors described the  $G'$  temperature dependence as a “two-step gelation”, attributed to the build-up of two phase-separated networks formed by  $\iota$ -carrageenan at higher temperatures and by  $\kappa$ -carrageenan at lower temperatures. The discrepancy between this nonmonotonic thermal behavior and the temperature sweeps depicted in Figure 1 (the thermal dependence of  $G'$  was checked to be equally monotonic) is in favor of a statistical distribution of blocks of  $\iota$ -carrageenan and  $\kappa$ -carrageenan monomers making up the present  $\kappa/\iota$ -hybrid carrageenan copolymer. Actually, such macromolecular architecture impedes the microphase separation of  $\kappa$ - and  $\iota$ -carrageenan monomers, and the formation of two phase-separated or interpenetrated networks is consequently forbidden. Alternatively, under the present salt and polymer concentration conditions, the network associated with  $\iota$ -carrageenan monomers is elastically far weaker than the network associated with  $\kappa$ -carrageenan monomers and cannot be resolved during the temperature sweeps. Indeed, for all concentration tested so far and ranging from 0.2% to 2.5% w/w (27), temperature sweeps with a single step in  $G'$  and  $G''$  have been recorded. However, experiments carried out with 0.1 mol/dm<sup>3</sup> NaCl salt and with biopolymer concentrations above 2% w/w (27) revealed that the  $\iota$ -carrageenan network shows up at high

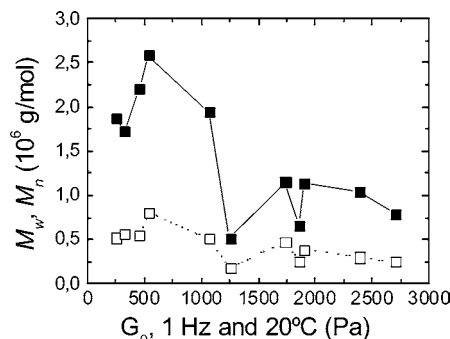


**Figure 7.**  $\kappa/\iota$ -Hybrid carrageenans molecular weights  $M_w$  (■) and  $M_n$  (◻) as a function of the corresponding equilibrium gels elastic modulus  $G_0$ .

temperatures (above 50 °C) as a kink in the otherwise monotonic temperature dependence of  $G'$ , prior to the development of the elastically stronger  $\kappa$ -carrageenan network.

**3.4. Correlation between Gel Elasticity and Molecular Weight Distribution.** A comparison between the molecular weight distributions (characterized by  $M_w$  and  $M_n$ ) of the  $\kappa/\iota$ -hybrid carrageenan biopolymers and the elastic modulus  $G_0$  of the corresponding gels is proposed in Figure 7. This representation clearly indicates that both  $M_w$  and  $M_n$  are decreasing functions of  $G_0$ . This result is rather surprising if one notes here that all  $M_w$  values are above the  $\kappa$ -carrageenan ideal homopolymer critical molecular weight beyond which gel elasticity shows no molecular weight dependence (28). This unexpected behavior can be understood by bearing in mind the copolymer nature of the  $\kappa/\iota$ -hybrid carrageenans. Indeed, a prerequisite for gel formation is the existence of blocks of pure  $\kappa$ -carrageenan or pure  $\iota$ -carrageenan monomers with lengths bigger than the critical one for helix formation. In a recent study (16), minimum lengths for helix formation have been calculated: these are eight or nine  $\kappa$ -carrageenan monomers and two or three  $\iota$ -carrageenan monomers. However, the presence of biological precursors may lead to a dramatic increase in this minimum length. The monomers in the  $\kappa/\iota$ -hybrid carrageenan macromolecular chain that do not participate in helix formation and subsequent aggregation will essentially act as free dangling chains, thereby causing a plasticizing effect to the gel network. As such, bigger  $\kappa/\iota$ -hybrid carrageenan molecular weights bring more free dangling chains to the gel structure, which exhibits inherent softer elasticity. One may conclude at that point (see below for a discussion of this result based on the statistical analysis of the data) that the gel elasticity of  $\kappa/\iota$ -hybrid carrageenans extracted from *M. stellatus* can be tuned by controlling the molecular weight of the polysaccharides. We showed in a previous study (20) that this control could be achieved by monitoring the extraction time: the longer the extraction duration, the shorter the resulting biopolymers, with no modification of the polysaccharide chemical structure.

**3.5. Relationships between Chemical Structure and Gel Mechanical Properties.** In an attempt to correlate the  $\kappa/\iota$ -hybrid carrageenan chemical structure to product functional properties such as gel elasticity, we systematically plot mechanically relevant chemical properties as a function of gels elasticity  $G_0$ . In Figure 8, the chemical characteristics determined with FTIR spectroscopy are compared to  $G_0$ . The degree of  $\kappa/\iota$  hybridization can be calculated by computing a FTIR band intensity ratio (22, 29): the 805 cm<sup>-1</sup> absorption band intensity over the 845 cm<sup>-1</sup> absorption band intensity. This ratio, hereafter denoted as  $\iota$ -content, can be seen as an indication of the relative amount of  $\iota$ -carrageenan monomers with respect to all other gelling and

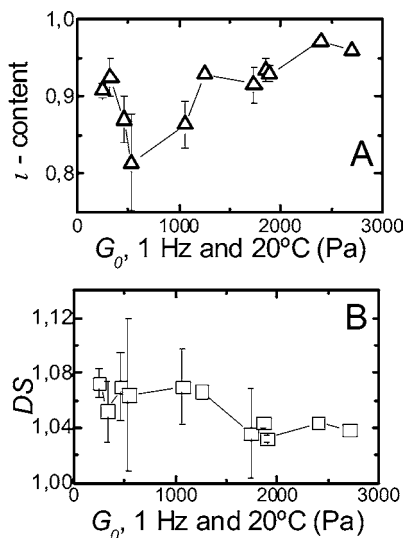


**Figure 8.** Relationship between  $\kappa/\lambda$ -hybrid carrageenan chemical structure as measured by FTIR spectroscopy and equilibrium gel elastic modulus  $G_0$ . (A)  $l$ -content as a function of  $G_0$ . (B) Degree of sulfate DS as a function of  $G_0$ .

nongelling carrageenan monomers in the polysaccharide. As such, and under the assumption of (i) a blockwise distribution of  $l$ -carrageenan monomers along the copolymer chain, (ii) the absence of correlations between the  $l$ -content and other elastically relevant parameters (see discussion below), and (iii) a gel elasticity solely arising from  $l$ -carrageenan monomers, the  $l$ -content is likely to be an increasing function of  $G_0$ . The  $l$ -content is plotted as a function of the gels elasticity  $G_0$  in **Figure 8A**. Despite some scattering in the data at low  $G_0$  values (softer gels), results suggest that a higher content in  $l$ -carrageenan monomers results in improved gel elastic properties. In a similar way, the degree of sulfate groups in the biopolymer (DS) is usually estimated from FTIR data (30) by computing the ratio of the band intensity at  $1250\text{ cm}^{-1}$  over the band intensity at  $2920\text{ cm}^{-1}$  (the latter corresponding to CH groups). Comparison of DS with gel elastic properties is relevant, since DS is a direct measure of the amount of nongelling carrageenan units in the polysaccharide. The increase in gel elasticity with decreasing values of DS is widely documented in the literature (1) for ideal  $\kappa$ - or  $l$ -carrageenan homopolymers and is explained by the fact that biological sulfated precursors locally stop the homopolymer stereochemical regularity (the blockwise distribution of gelling monomers is interrupted by nongelling monomers), thus restricting the polysaccharide conformational transition from coil to aggregating helices (2). However, due to spectral width limitations in our FTIR data (absorptions were recorded between 600 and  $1400\text{ cm}^{-1}$ ), we are prompted to propose the ratio between the band intensity at  $1250\text{ cm}^{-1}$  and the band intensity measured at  $930\text{ cm}^{-1}$ , as an alternative to the estimation of DS. The use of the band showing up at  $930\text{ cm}^{-1}$  is motivated by the fact that the latter is specific to less sulfated  $\kappa$ - and  $l$ -carrageenan monomers (4, 22, 23). The new ratio DS is plotted in **Figure 8B**, again as a function of  $G_0$ . As expected, data indicate that more elastic gels are obtained for  $\kappa/\lambda$ -hybrid carrageenans bearing less sulfated groups and thus validate the use of the proposed DS calculation.

A comparison between  $^1\text{H}$  NMR quantitative analysis and  $G_0$  is summarized in **Figure 9**. The  $^1\text{H}$  NMR analysis relies on the computation of ratios of peak intensities (integrated areas) assigned to a specific carrageenan monomer over the sum of all peak intensities considered in the analysis. For instance, the relative content in  $\kappa$ -carrageenan monomers is obtained from

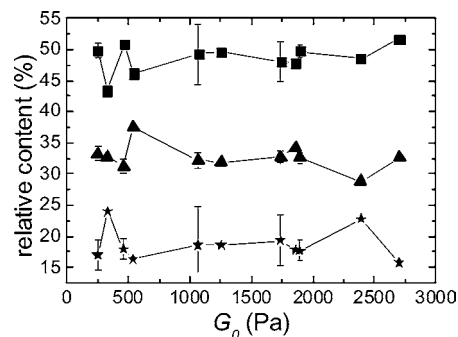


**Figure 9.** Relationship between  $\kappa/\lambda$ -hybrid carrageenan chemical structure as measured by  $^1\text{H}$  NMR spectroscopy and gel elastic modulus  $G_0$ : relative content of  $\kappa$ -carrageenan monomers (■),  $l$ -carrageenan monomers (▲), and biological precursor monomers (□).

the ratio of the peak intensity measured at 5.11 ppm over the sum of peak intensities recorded at 5.11, 5.32 (for  $l$ -carrageenan monomers), 5.52 (for  $\nu$ -carrageenan monomers) and 5.26 ppm (for  $\mu$ -carrageenan monomers). Data gathered in **Figure 9** show that the  $^1\text{H}$  NMR peak intensity ratio giving the relative content in  $\kappa$ -carrageenan monomers is roughly an increasing function of  $G_0$ , if data scattering at low  $G_0$  is neglected: relative content ranges from 43% (softer gels) to 52% (stronger gels) for a corresponding 10-fold increase in gel elasticity ( $G_0$  increases from 250 to 2700 Pa). A recent study (16) on a series of  $\kappa/\lambda$ -hybrid carrageenans extracted from different seaweeds and containing from 60% to 100%  $\kappa$ -carrageenan monomers with less than 2% nongelling monomers showed a very similar relationship between the gels elasticity and the relative content in  $\kappa$ -carrageenan monomers. In contrast to that, peak intensity ratios computed for both  $l$ -carrageenan and biological carrageenan precursor monomers  $\nu$  and  $\mu$  (the latter ratio is obtained by summing the ratios corresponding to  $\nu$ -carrageenan and  $\mu$ -carrageenan monomers) and displayed in **Figure 9** are virtually not depending on  $G_0$ . Poor NMR detection sensitivity (peak relative intensity ranging from 5 to 10% for  $\nu$ -carrageenan monomers) is apparently responsible for the appreciable lack of correlation between  $G_0$  and the relative content in biological carrageenan precursor monomers. Note here that, in the light of the discussion developed above for DS, depressed gel elasticity should correlate with polysaccharides containing more biological precursors. The nondependence of  $l$ -carrageenan monomers relative content on gel elastic properties is more questionable, as this result is hard to reconcile with the  $l$ -content measured with FTIR spectroscopy (see **Figure 8**). Actually, both chemical analyses should render the same experimental output, as both spectroscopic methods assess the same chemical property. A plausible reason for the absence of consistent results might again lie in the poor  $^1\text{H}$  NMR quantitative sensitivity to small amounts of biological precursors, which hampers the interpretation of computed peak intensity ratios. In particular,  $\mu$ -carrageenan monomers show up as a shoulder to the  $l$ -carrageenan peak in the  $^1\text{H}$  NMR line shape (see **Figure 2**), thus posing serious limitations to a correct quantitative measure of respective signals intensities. In the light of the results presented above, it seems that for the peculiar case of *M. stellatus* seaweeds, a quantitative analysis of the biopolymers chemical structure is better achieved by means of FTIR spectroscopy, since the latter technique produces chemical parameters that reliably correlate with the elastic properties of  $\kappa/\lambda$ -hybrid carrageenan gels.

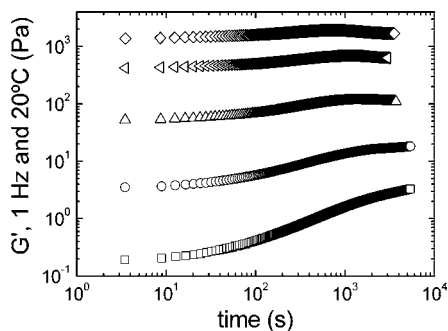


**Figure 10.** Time dependence of the storage modulus  $G'$  measured at 1 Hz and 20 °C during the equilibration of gels obtained for different concentrations of sample M25 in 0.05 mol/dm<sup>3</sup> KCl: (□) 0.2% w/w; (○) 0.3% w/w; (△) 0.5% w/w; (◻) 0.9% w/w; (◇) 1.3% w/w.

#### 4. DISCUSSION

The time evolution of the storage modulus  $G'$  shows a maximum as the gel progresses toward its mechanical equilibrium. Before providing an interpretation for this maximum, a check for possible experimental artifacts first needs to be carried out. It is worth noting here that gel kinetics similar to the ones displayed in **Figures 1, 3, and 4** have been systematically observed for all biopolymers listed in **Table 1** and for all sample thicknesses (ranging from 0.8 mm to 1 mm) used throughout this study. In addition, a maximum in  $G'$  was also resolved in tests performed with a cone and plate geometry: both maximum amplitude and time location showed good reproducibility with tests performed with smooth plates. The use of excessive strain as a possible source for experimental error has been suggested above, and Fourier transform analysis of both torque and strain signals has been performed to establish the absence of strain-induced structural rearrangements within the gels. As an ultimate check, experiments depicted in **Figure 1A,B** have been reproduced with the strain set to 0. The mechanical spectrum of the gel obtained after this sample treatment showed a satisfactory reproducibility ( $G'$  and  $G''$  values differing by less than 15%) when compared to data displayed in **Figure 1C**: this result confirms that strain-induced structural rearrangement is not related with the observed gel kinetics. The latter is rather the signature of a structural property of carrageenan gels (6) and should therefore depend on parameters such as the biopolymer concentration. Preliminary studies are presented in **Figure 10**, where the time dependence of  $G'$  is plotted for five different concentrations of biopolymers solutions obtained with sample M25 (the latter showed the best gelling properties of the  $\kappa/\iota$ -hybrid carrageenans studied here). For concentrations below 0.5% w/w,  $G'$  exhibits a monotonic increase before reaching an equilibrium plateau. This gel kinetics is reminiscent from the one obtained some time ago for  $\kappa$ -carrageenan solutions with similar concentrations (9). When the concentration is raised above 0.5% w/w, the  $G'$  maximum is resolved. The latter appears at earlier times in the gel kinetics and with increased amplitude as the concentration is increased. The maximum time location and amplitude also depend on the cooling rate used to set the gel (results not shown): a bigger maximum occurs at earlier times if the cooling rate is slower. These features suggest that aggregation phenomena are involved in the intrinsic structural rearrangement of the gel. As the temperature is lowered, helices are formed and aggregate in bundles of helices (1, 6–8). These bundles act as cross-links between the remaining parts of macromolecules that did not adopt a helix conformation, as biological precursor monomers limit the extent of conformational transition (5, 16). As time proceeds, more bundles are

**Table 2.** Correlation Coefficients between  $G'$  Maximum Amplitude (MAX) and Time Location (TIME) and Gel Thermal Parameters ( $T_m$ ,  $T_g$ ,  $\Delta T$ ) Measured for All Samples Listed in **Table 1**

	MAX	TIME	$T_m$	$T_g$	$\Delta T$
MAX	1	−0.2	−0.4	−0.38	−0.37
TIME		1	0.23	0.36	0.08
$T_m$			1	0.92	0.94
$T_g$				1	0.73
$\Delta T$					1

formed, thereby increasing the cross-link density in the forming gel. Consequently, the gel elasticity rises and the time evolution of the storage modulus  $G'$  witnesses this structural build-up. At longer times, the bundles are merging as helix aggregation proceeds, resulting in a decrease in cross-link density, which is mirrored by the decrease in  $G'$ . As such, a maximum in the storage modulus is expected to show up during the gel kinetics. A simple way to validate this structural picture is to look for correlations between the maximum amplitude or time location and parameters such as  $T_m$  or  $\Delta T$ , which are known to be related to aggregation (10, 11). Such a statistical analysis is provided in **Table 2**, where linear correlation coefficients computed with the Statistica software, version 6.1 (Statsoft, Tulsa, OK), are reproduced. The rather low values of the coefficients in **Table 2** indicate that the kinetics of gel rigidity does not correlate with the gel melting behavior or gel thermal hysteresis, suggesting that bundles of helices are not the only structural units that contribute to gel elasticity. Clearly, additional work including in situ structural characterization is needed if one wants to provide a better understanding of  $G'$  maximum, as no further correlations between the maximum amplitude or time location and  $\kappa/\iota$ -hybrid carrageenans chemical composition, molecular weight distribution, and equilibrium elastic modulus  $G_0$  could be evidenced.

Gels obtained from  $\kappa/\iota$ -hybrid carrageenans exhibit an equilibrium elastic modulus  $G_0$  that is related to gel thermal properties (see **Figure 6**). Moreover,  $G_0$  depends on the molecular weight distribution (see **Figure 7**) and on the biopolymer chemical composition as determined by FTIR experiments (see **Figure 8**). A tentative interpretation has been given for each of these results, namely, helix aggregation and tridimensional networking, free dangling chains acting as gel plasticizers, and biological precursor monomers that limit the extent of helix formation and subsequent aggregation. These interpretations are partly motivated by earlier reports on virtual model carrageenan systems (1–3, 5–12, 14–16) and are based on the hypothesis that  $G_0$  solely depends on the parameter under study, whereas all the others are either kept constant or are simply not correlated with the studied parameter or physical property. The  $\kappa/\iota$ -hybrid carrageenans extraction process (20) results in a set of samples that vary by more than one parameter. Therefore, statistical analysis of the correlations between all elastically relevant parameters ( $T_g$ , molecular weight distribution and chemical composition) is required in order to discern their respective impact on  $G_0$  and validate the above-mentioned interpretation or alternatively underpin their complex interplay with  $G_0$ . The results of the statistical analysis (performed as mentioned above) of data presented in **Figures 6–9** are displayed in **Table 3**, where linear correlation coefficients between all studied parameters are reported. The gel-setting temperature  $T_g$  is not correlated with any chemical parameters nor with the molecular weight distribution, since corresponding coefficients are kept between −0.59 and 0.36. Thus, the dependence of  $G_0$  on chemical parameters and on  $M_w$  or  $M_n$

**Table 3.** Correlation Coefficients between Gel Physical Parameters ( $T_m$ ,  $T_g$ ,  $\Delta T$ ,  $G_0$ ) and Biopolymers Chemical Parameters ( $M_w$ ,  $M_n$ , DS,  $\iota$ -content,  $\iota$ ,  $\kappa$ , PREC) Measured for All Samples Listed in Table 1

	$T_m$	$T_g$	$\Delta T$	$G_0$	$M_w$	$M_n$	DS	$\iota$ -content	$\iota^a$	$\kappa^a$	PREC <sup>a</sup>
$T_m$	1	0.92	0.94	0.87	-0.72	-0.69	-0.6	0.49	-0.26	0.35	-0.11
$T_g$		1	0.73	0.74	-0.59	-0.52	-0.45	0.3	-0.1	0.31	-0.19
$\Delta T$			1	0.87	-0.74	-0.74	-0.65	0.6	-0.36	0.35	-0.01
$G_0$				1	-0.75	-0.71	-0.77	0.69	-0.36	0.4	-0.06
$M_w$					1	0.95	0.58	-0.84	0.4	-0.27	-0.09
$M_n$						1	0.4	-0.83	0.56	-0.47	-0.04
DS							1	-0.62	0.13	0.04	-0.15
$\iota$ -content								1	-0.63	0.19	0.36
$\iota$									1	-0.35	-0.52
$\kappa$										1	-0.62
PREC											1

<sup>a</sup>  $\iota$ ,  $\kappa$ , and PREC stand for the relative contents in  $\iota$ -monomers,  $\kappa$ -monomers, and biological precursor monomers, respectively, as determined by <sup>1</sup>H NMR and plotted in Figure 9.

will not be blurred by its dependence on  $T_g$ . The molecular weight distribution is strongly correlated with the content in  $\iota$ -carrageenan monomers as determined by FTIR (coefficients of -0.84 and -0.83 for parameters  $M_w$  and  $M_n$ , respectively). This suggests that longer  $\kappa/\iota$ -hybrid carrageenan macromolecules possess proportionally less  $\iota$ -carrageenan monomers. Unfortunately, chemical parameters, which were obtained from <sup>1</sup>H NMR spectra (with inherently big data scattering and experimental errors as evidenced in Figure 9 and explained in the Results section) are not correlated with either  $M_w$  or  $M_n$ . This analysis thus cannot indicate if absent  $\iota$ -carrageenan monomers in longer biopolymers chains are substituted by  $\kappa$ -carrageenan monomers or rather nongelling units, which would favor the occurrence of free dangling chains in the gels. A way to overcome this lack of information is to focus now on the thermal hysteresis  $\Delta T$ , which reflects the extent of aggregation of helices in the gels.  $\Delta T$  becomes smaller as the molecular weight is bigger (correlation coefficients are truly negative for both  $M_w$  and  $M_n$  parameters), which suggests that long  $\kappa/\iota$ -hybrid carrageenan chains form less aggregates because they contain relatively less helical conformers, whereas shorter biopolymers contain relatively more helices. A final comment deals with the increased gel elasticity  $G_0$  with the increasing relative content in  $\iota$ -carrageenan monomers, as depicted in Figure 8. This positive correlation (the corresponding coefficient reads 0.69 in Table 3) is difficult to reconcile with the  $\kappa/\iota$ -hybrid carrageenan gel elasticity, which seems rather dominated by a  $\kappa$ -carrageenan-like behavior as mentioned earlier: gel kinetics is slow and presents a maximum in  $G'$ , mechanical spectra qualitatively resemble that of pure  $\kappa$ -carrageenan gels, and both  $\Delta T$  and  $G_0$  values are seemingly bigger than those found in pure  $\iota$ -carrageenan gels under similar salt and concentration conditions (27). As mentioned earlier, the  $\iota$ -content is not an independent parameter, as it strongly correlates with the molecular weight distribution. Therefore, it does not allow the simple rationalization provided in the Results section and based on too strong or unverified assumptions.

#### ACKNOWLEDGMENT

The authors gratefully acknowledge Prof. Pedro Abreu and Prof. Ana M. Ramos (REQUIMTE-CQFB, Lisboa) for performing the FTIR, <sup>1</sup>H NMR, and size exclusion chromatography experiments.

#### LITERATURE CITED

- Piculell, L. Gelling carrageenans. In *Food Polysaccharides and Their Applications*; Stephen A. M., Ed.; Marcel Dekker Inc.: New York, 1995; pp 205–244.
- Van de Velde, F.; Knutsen, S. H.; Usov, A. I.; Rollema, H. S.; Cerezo, A. S. <sup>1</sup>H and <sup>13</sup>C high resolution MNR spectroscopy of carrageenans: Application in research and industry. *Trends Food Sci. Tech.* **2002**, *13*, 73–92.
- Lahaye, M. Developments on gelling algal galactans, their structure and physico-chemistry. *J. Appl. Phycol.* **2001**, *13*, 173–184.
- Chopin, T.; Kerin, B. F.; Mazerolle, R. Phycocolloid chemistry as a taxonomic indicator of phylogeny in the Gigartinales, Rhodophyceae: A review and current developments using Fourier transform infrared diffuse reflectance spectroscopy. *Phycol. Res.* **1999**, *47*, 167–188.
- Van de Velde, F.; Rollema, H. S.; Grinberg, N. V.; Burova, T. V.; Grinberg, V. Y.; Tromp, R. H. Coil-helix transition of  $\iota$ -carrageenan as a function of chain regularity. *Biopolymers* **2002**, *65*, 299–312.
- Hermansson, A. M. Rheological and microstructural evidence for transient states during gelation of kappa-carrageenan in the presence of potassium. *Carbohydr. Polym.* **1989**, *10*, 163–181.
- MacArtain, P.; Jacquier, J. C.; Dawson, K. A. Physical characteristics of calcium induced  $\kappa$ -carrageenan networks. *Carbohydr. Polym.* **2003**, *53*, 395–400.
- Ikeda, S.; Morris, V. J.; Nishinari, K. Microstructure of aggregated and non aggregated  $\kappa$ -carrageenan helices visualized by atomic force microscopy. *Biomacromolecules* **2001**, *2*, 1331–1337.
- Meunier, V.; Nicolai, T.; Durand, D.; Parker, A. Light scattering and viscoelasticity of aggregating and gelling  $\kappa$ -carrageenan. *Macromolecules* **1999**, *32*, 2610–2616.
- Ikeda, S.; Kumagai, H. Dielectric analysis of sol-gel transition of  $\kappa$ -carrageenan with scaling concept. *J. Agric. Food Chem.* **1998**, *46*, 3687–3693.
- Takemasa, M.; Chiba, A.; Date, M. Gelation mechanism of  $\kappa$ - and  $\iota$ -carrageenan investigated by correlation between the strain-optical coefficient and the dynamic shear modulus. *Macromolecules* **2001**, *34*, 7427–7434.
- Ikeda, S.; Nishinari, K. “Weak gel” type rheological properties of aqueous dispersions of nonaggregated  $\kappa$ -carrageenan helices. *J. Agric. Food Chem.* **2001**, *49*, 4436–4441.
- Hossain, K. S.; Miyana, K.; Maeda, H.; Nemoto, N. Sol-gel transition behaviour of pure  $\iota$ -carrageenan in both salt-free and added salt states. *Biomacromolecules* **2001**, *2*, 442–449.
- van de Velde, F.; Peppelman, H. A.; Rollema, H. S.; Tromp, R. H. On the structure of  $\kappa/\iota$ -hybrid carrageenans. *Carbohydr. Res.* **2001**, *331*, 271–283.
- Falshaw, R.; Bixler, H. J.; Johndro, K. Structure and property of commercial kappa-2 carrageenan extracts I. Structure analysis. *Food Hydrocolloid* **2001**, *15*, 441–452.
- Van de Velde, F.; Antipova, A. S.; Rollema, H. S.; Burova, T. V.; Grinberg, N. V.; Pereira, L.; Gilson, P. M.; Tromp, R. H.; Rudolph, B.; Grinberg, V. Y. The structure of  $\kappa/\iota$ -hybrid carrageenans II. Coil-helix transition as a function of chain composition. *Carbohydr. Res.* **2005**, *340*, 1113–1129.
- Chanvrier, H.; Durand, S.; Garnier, C.; Sworn, G.; Bourriot, S.; Doublier, J. L. Gelation behaviour and rheological properties of  $\kappa/\iota$  hybrid carrageenans. In *Gums and Stabilisers for the Food Industry*; Williams, P. A., Phillips, G. O., Eds; The Royal Society of Chemistry: Cambridge, 2004; Vol. 12, pp 139–145.
- Bixler, H. J.; Johndro, K.; Falshaw, R. Kappa-2 carrageenan: Structure and performance of commercial extracts II. Performance in two simulated dairy applications. *Food Hydrocolloid* **2001**, *15*, 619–630.



- (19) Villanueva, R. D.; Mendoza, W. G.; Rodriguez, M. R. C.; Romero, J. B.; Montaña, M. N. E. Structure and functional performance of gigartinacean kappa-iota hybrid carrageenan and solieriacean kappa-iota carrageenan blends. *Food Hydrocolloid* **2004**, *18*, 283–292.
- (20) Hilliou, L.; Larotonda, F. D. S.; Abreu, P.; Ramos, A. M.; Sereno, A. M.; Gonçalves, M. P. Effect of extraction parameters on the chemical structure and gel properties of  $\kappa/\iota$ -hybrid carrageenans obtained from *Mastocarpus stellatus*. *Biomol. Eng.* **2006**, in print.
- (21) Winter, H. H.; Mours, M. Rheology of polymers near liquid-solid transitions. *Adv. Polym. Sci.* **1997**, *134*, 165–234.
- (22) Pereira, L.; Mesquita, J. F. Carrageenophytes of occidental Portuguese coast: I—Spectroscopic analysis in eight carrageenophytes from Buarcos Bay. *Biomol. Eng.* **2003**, *20*, 217–222.
- (23) Volery, P.; Besson, R.; Schaffer-Lequart, C. Characterization of commercial carrageenans by Fourier transform infrared spectroscopy using single-reflection attenuated total reflection. *J. Agric. Food Chem.* **2004**, *52*, 7457–7463.
- (24) Parker, A.; Brigand, G.; Miniou, C.; Trespoey, A.; Vallée, P. Rheology and fracture of mixed  $\iota$ - and  $\kappa$ -carrageenan gels: Two-step gelation. *Carbohydr. Polym.* **1993**, *20*, 253–262.
- (25) Hermansson, A. M.; Eriksson, E.; Jordansson, E. Effects of potassium, sodium and calcium on the microstructure and rheological behaviour of kappa-carrageenan gels. *Carbohydr. Polym.* **1991**, *16*, 297–320.
- (26) Wilhelm, M. Fourier-transform rheology. *Macromol. Mater. Eng.* **2002**, *287*, 83–105.
- (27) Hilliou, L.; Gonçalves, M. P. Gelling properties of a  $\kappa/\iota$ -hybrid carrageenan: Effect of salt, concentration and steady shear. *Proceedings of the 4th International Symposium on Food Rheology and Structure, Zurich, Switzerland, Feb 20–23, 2006*; Fischer, P., Erni, P., Windhab, E. J., Eds; Kerschensteiner Verlag: Lappersdorf, 2006.
- (28) Rochas, C.; Rinaudo, M.; Landry, S. Role of molecular weight on the mechanical properties of  $\kappa$ -carrageenan gels. *Carbohydr. Polym.* **1990**, *12*, 255–266.
- (29) McCandless, E. L.; West, J. A.; Guiry, M. D. Carrageenan patterns in the Gigartinaceae. *Biochem. Syst. Ecol.* **1983**, *11*, 175–182.
- (30) Rochas, C.; Lahaye, M.; Yaphe, W. Sulfate content of carrageenan and agar determined by infrared-spectroscopy. *Bot. Mar.* **1986**, *29*, 335–340.

---

Received for review May 8, 2006. Revised manuscript received July 28, 2006. Accepted August 11, 2006. This work was supported by the Fundação para a Ciência e a Tecnologia (project POCTI/EQU/45595/2002). F.D.S.L. received a scholarship award (E04D027282BR) from the Programme Alban, the European Union Programme of High Level Scholarships for Latin America.

JF0612934